JOM, Vol. 75, No. 7, 2023
https://doi.org/10.1007/s11837-023-05889-1

Electrically Assisted Vat Photopolymerization of Bioinspired Hierarchical Structures with Controllable Roughness for Hydrophobicity Enhancement Using Photocurable Resin/Carbon Nanotube

TENGTENG TANG,[1] GANA SAI KIRAN AVINASH RAJ DWARAMPUDI,[1] and XIANGJIA LI [1,2]

1.—Department of Aerospace and Mechanical Engineering, School for Engineering of Matter, Transport and Energy, Arizona State University, 501 E. Tyler Mall, Tempe, AZ 85287, USA. 2.—e-mail: xiangjia.li@asu.edu

The superhydrophobic properties of *Salvinia molesta* are observed to prevent wetting and submersion in water. Replicating this structure has always been highly desired because of its excellent superhydrophobicity but has been constrained by existing fabrication methods. Here, we proposed an electrically assisted vat photopolymerization (e-VPP) to control the surface roughness of Salvinia-inspired structures at the micro- and nanoscale through the introduction of multiwalled carbon nanotubes (MWCNTs). Experimental results show that using MWCNTs increases the superhydrophobic properties of printed bioinspired structures at a relatively high concentration compared to the normal pure resins. Alignment of MWCNTs also boosts overall performance of biomimetic structures, such as mechanical strength, contact angle and liquid surface attaching forces. Thus, these outputs make it possible to achieve better interfacial performance with controllable micro-/nano-dual-scale surface roughness properties by adjusting material composition and distribution for multiple applications, such as droplet control, micro-droplet reactor, microdroplet non-loss transportation, anti-bacteria surface, water robot and oil–water separation.

INTRODUCTION

Over millions of years of evolution, natural organisms have gained complex hierarchical architectures with highly integrated structure and function, which open up an unprecedented path for the design and manufacture of high-performance functional devices, especially hydrophobicity.[1,2] The eggbeater-like structures of *Salvinia molesta*, the floating leaves of water fern, demonstrate superhydrophobicity, which helps the water droplet to stay afloat on the leaves (Fig. 1a,b).[3,4] The microscale eggbeater-shaped hairs are decorated with microscopic granules and nanoscopic wax crystals (dual-scale roughness), and wrinkled hydrophilic patches without wax crystals are evenly distributed on the terminal of each hair (Fig. 1c).[5] In some of the previous studies, these *Salvinia*-based biomimetic structures have been made using different photocurable resins. Although it is difficult to increase the surface roughness properties at multiscale only using the resin, it is much easier to adjust the printing parameters to achieve macroscale roughness. The size, number of eggbeater arms and gap distance between pillars were all variable so it was possible to examine how they affected the hydrophobic property and water adhesion. Notably, the multiscale roughness at microscale level is easy to achieve but nanoscale wax-crystal-like roughness is difficult to obtain without any fillers. The

(Received January 30, 2023; accepted April 28, 2023; published online May 22, 2023)

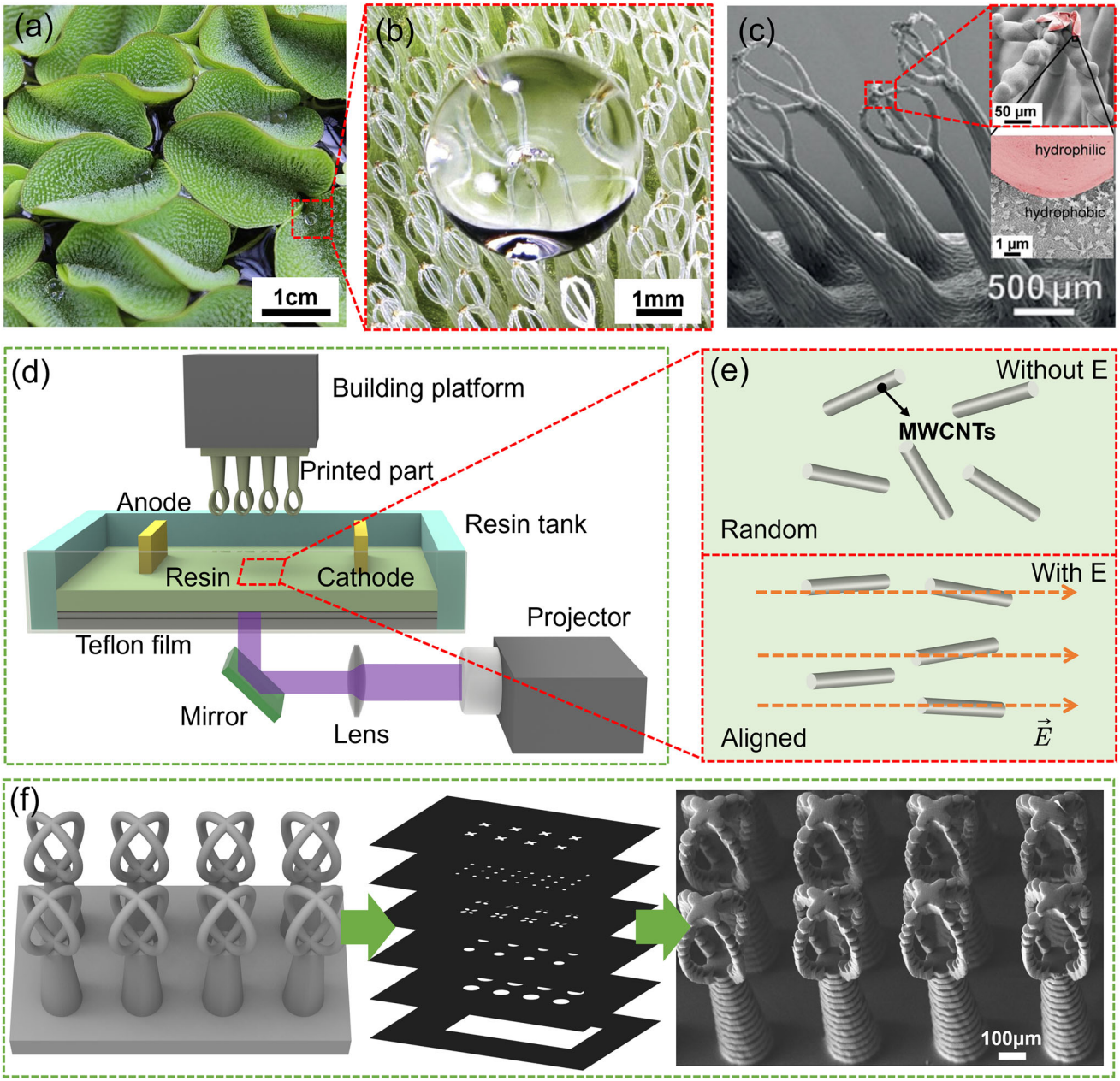

Fig. 1. Bioinspired design and manufacturing process. (a) *Salvinia molesta* leaf in nature, reprinted from Ref. 31 under the terms of Creative Commons Attribution-Share Alike 3.0 Unported license. (b) Microstructures on leaf surfaces support water droplets, reprinted from Ref. 32 under the terms of Creative Commons CC BY license. (c) Scanning electron microscope (SEM) image of eggbeater microstructures with dual-scale roughness; the main image is reprinted with permission from Ref. 3, and the two subplots in the upper right corner are reprinted from Ref. 32 under the terms of Creative Commons CC BY license. (d) Schematic diagram of electrically assisted vat photopolymerization set-up. (e) MWCNTs aligned under electrical field. (f) Illustration of the fabrication process of printing eggbeater microstructure.

hypothesis is that the MWCNTs were additionally included in the liquid resin to both improve surface roughness at micro-scale and eliminate static charges generated on surfaces with its high-conductive nature. Also, the electrical properties help in their alignment when exposed under electric field, and both the chemical composition and geometric structure of an eggbeater surface influence its unique wetting properties.[6]

A stable and continuous voltage source is used to regulate the alignment of MWCNTs, and it is investigated how to employ this external control to provide superior mechanical characteristics. Due to their distinctive structural characteristics and excellent mechanical qualities, MWCNTs have shown significant promise as multifunctional nanofillers for polymer-based nanocomposites. To further enhance the multifunctional characteristics,

controlled alignment of MWCNTs in polymer matrix by electric field is studied, which helps obtain better roughness properties at nanoscale. Thus, superhydrophobic structures with multi-scale roughness, at micro-scale due to the dispersion of MWCNTs and at nano-scale due to the alignment of MWCNTs, can be achieved. The endeavor to replicate nature-inspired structures poses a significant challenge, primarily attributed to the intricate interplay of multiple factors such as high precision, dual-scale integration spanning the micro- and nano-levels and stringent environmental considerations. Although extensive research has been carried out, traditional manufacturing methods such as molding, coating and deposition are far from meeting the requirements of the fabrication of superhydrophobic surfaces.[7,8] Benefit is derived from the newly emerging additive manufacturing (AM) technologies and widely available materials;[9,10] AM expands its capability from primitive prototype verification to fabricating highly functional devices, specifically bioinspired superhydrophobic structures.[11,12] Nevertheless, current 3D-printed bioinspired surfaces[13,14] have encountered bottlenecks in reproducing such dual-scale roughness, and the performances of printed structures still cannot achieve the same liquid-repellent and air trapping capability as natural structures.[15,16]

Here, we proposed an electrically assisted 3D printing method of bioinspired hierarchical structures with controllable roughness for hydrophobicity enhancement. In our study, the controllable surface roughness and wettability will be achieved by using multi-wall carbon nanotube (MWCNT)-based nanocomposite for the 3D printing of multi-scale, bioinspired, eggbeater-shaped structures so that stable and long-term air retention can be achieved in large dimensions.[17] Digital light processing (DLP)[18] is a novel AM process where the horizontally sliced images of the structure are projected to the one after the other on the photocurable resin to create a photopolymerized structure.[19] The layer-by-layer printing process helps to create a structure with controlled micro-scale surface roughness, which is difficult to control using traditional methods. To fabricate a hierarchical structure that is structurally strong and possesses nanoscale roughness, the MWCNTs are added to the resin and aligned in a specific direction. The directionality of the MWCNTs is determined by the electric field and fixed with the cured resin, which further helps to improve the structural hydrophobicity and mechanical performance.[20] Printed structures are tested from the aspect of wettability, attaching forces, contact angle and structural strength. Thus, the bioinspired hierarchical structures consisting of microscale superhydrophobic hair with dual-scale roughness and wrinkled hydrophilic patches can be achieved with the help of biomimicry[21] and novel electrically assisted 3D printing technique. We believe that its '*Salvinia* effect' can be applied in the field like water wheel propeller, anisotropic water transport,[22,23] water/oil separation and dispersion/separation of polar and non-polar substances[24] for biomedical devices.[25,26]

MATERIALS AND METHODS

MakerJuice SF Red Resin was purchased from MatterHackers. MWCNTs were purchased from Sigma-Aldrich. Two mixing methods are used to prepare the mixture with different weight percentages of MWCNTs: (1) vortex mixing for 5 min; (2) magnetic stirring mixing at 400 rpm for 30 min. All mixtures are vacuumed to remove air bubbles prior to printing.

During the printing, the images are projected one at a time from the projector onto the bottom surface of the vat tank after the CAD model has been segmented into slices for VPP (Fig. 1f). The self-developed program that projects mask images onto the bottom surface of the vat tank uses a set of sliced mask images. The exposure time, number of layers to print, building platform's travel distance, layer thickness and images to project are all controlled by the programming software. As a result, the first layer is printed on the building platform's bottom surface after the first image has been projected onto the photopolymer resin. Based on the layer thickness specified, the building platform is then raised to create a new layer and lowered in a control motion to allow more resin in between for the following layers. Then, a structure is printed following several iterations. Throughout the project, curing times for the material are tracked using UV projector (405-nm wavelength). A shutter connected to a stepping motor is used to block the light to prevent overcuring between individual layers (extra light from the projector during the motion breaks). It is programmed to open when the image is projected and close based on the exposure time after the projection. As an illustration, we established specific parameters to produce eggbeater-shaped structures utilizing a composite of 0.5 wt.% MWCNTs. Each layer's exposure time and thickness were set to 0.5 s and 25 μm, respectively. The process of linear motion for preparing a new layer of liquid takes 30 s per layer, and aligning the MWCNTs for the last ten layers requires 15 s per layer under 2 kV. As a result, the entire printing procedure takes approximately 18 min.

For the measurement of the contact angle, a syringe needle was used to add a water droplet to the surface. The droplet maintains its circular form on the surface. An optical microscope was used to capture a side view photo of the produced droplet, which was then imported into ImageJ software for contact angle measurement. The morphological image of the printed eggbeater structure was taken by JEOL JXA-8530F electron microprobe analyzer.

The surface roughness of the printing sample in the single layer was characterized by ZeScope profilometer.

RESULTS AND DISCUSSION

Electrically Assisted Vat Photopolymerization

Vat photopolymerization[27,28] is a technique used in 3D printing. Photopolymerization process emits UV light onto liquid polymer resin to convert that liquid resin to solid.[29] In vat photopolymerization process (Fig. 1d),[30] a transparent tank is filled with liquid resin and is positioned so that the UV light is emitted onto the bottom surface of the resin. The vat tank is set with two copper electrodes (Fig. 1d) facing each other that are connected to an AC high-voltage source. The electric field is used to align the MWCNTs presented in the photopolymer resin. After curing one layer, the cured layer is lifted and then lowered on to the bottom surface of the tank with a new gap layer. This process is continued until the structure is completely printed and finished. In between the layers, there will be a time gap, time taken by the guide tool to lift the printed portion and come back to the bottom of the tank. The UV light coming from the projector in these intervals can cure the resin to some extent. This causes irregular strands of cured resin in between the printed structures and is difficult to clean. This problem is better avoided by using a stepped motor operated shutter that helps block the UV light in time interval between each layer. The immersed electrode set-up inside the resin is connected to an AC high-voltage output, where the voltage parameters can be altered (Fig. 1e). As a result, the e-VPP process is used with the help of electric field to align highly conductive materials like MWCNTs, which are added as nanofillers to the photopolymer resin that will be cured to print solid structures.

The 15 × 15-mm building platform is made of the same MakerJuice resin because it is used in the electric field and improves adhesion between the new prints and the platform surface. To improve adherence with freshly printed parts, the platform surface is roughened with a flat file after each print. The regulated speed, which is based on the number of layers to be printed, determines how quickly the platform lifts and lowers for each cycle. Here, the platform is raised ten layers of 5 μm thickness, or 500 μm, with a speed of 50 μm/s for each individual image projected. By doing so, the shape of the structure that will be printed can be controlled, and the printed layers can be raised without being damaged. These prints' surface roughness is always influenced by printing speed and print layer depth. Like other 3D printing processes, the shape of the structure improves with slower printing speeds. The mixture and its curing properties have a direct effect on the layer depth and exposure time. All other printing parameters remain constant while the MWCNTs present in the photocurable resin are aligned utilizing an electric field. High voltages are connected to the electrodes using the Hipot Tester. The platform is set to sleep state for a period of time to allow MWCNTs to start aligning at these voltages. When using the Hipot Tester, the set-up is unaltered. If these AC high voltages are continuously applied to the resin mixtures, the MWCNTs adopt the structure of a long chain. When current begins to flow through them, the Hipot Tester will shut off promptly. Hipot tester must be turned off after printing is complete before moving on to the next step. To print these eggbeaters using e-VPP 3D printing, a vat tank of 35 mm diameter is filled with the MWCNT mixed resin. After the printing process, a flat base with a thickness of 400 μm is created so that the eggbeaters can stand upon it. Next, the eggbeaters' stems and then the smallest component, the eggbeater heads, which have a size of 50 μm each, are printed. Because this method of production is bottom-up, the printed parts are adhered to the flat surface in the reverse direction and must be peeled off the tool for additional testing. The printed item has a rectangular base with a total size of 11 × 9 mm, with a 400-μm-thick base, and a total height of 1.75 mm. After the printing is finished, the printed part is cleaned in ultrasonic bath for 3–5 min for the excessive resin to wash off, and then it is dried for further tests.

Curing Characterization

Curing time is the amount of time needed for the photopolymerization of the polymer resin into solid. The resin cures more quickly or more slowly depending on the nanofiller added to it. MWCNTs are added to the polymer resin, which shatters the energy that is emitted by UV light. When exposed to an electric field, the MWCNTs create microscale MWCNT strands that align in a horizontal line and allow more projected UV light beams to initiate the photopolymerization process of the photocurable resin. Due to the tightly packed bundles that are next to one another, this MWCNT accumulation, which is perpendicular to the 2D light beam, causes greater light penetration. A relationship was developed to calculate the cure depth C_d of the photocurable resin using the light penetration, volume percentage and total energy. The following equation, developed by Griffith and Halloran, could be used to predict the curing model of MWCNT-based resin during the e-VPP process:[33]

$$C_d = \left(\frac{\eta_0}{\eta_P - \eta_0}\right)\frac{\lambda^2}{D}\ln\left(\frac{t}{t_c}\right)\frac{1}{\phi} \quad (1)$$

where η_0 is the refractive index of the photocurable resin, η_P is the refractive index of the MWCNT, λ is the wavelength of incident light, D is diameter of the MWCNT-based bundle, t is the exposure time, t_c is the critical exposure time, and ϕ is the concentration of MWCNTs in the mixture.

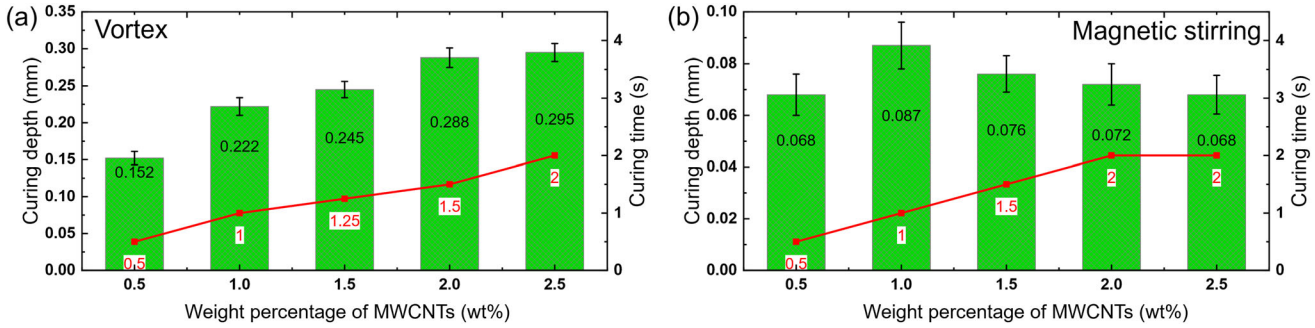

Fig. 2. Effect of dispersion conditions on curing properties of randomly distributed MWCNTs. (a) The curing characterization of the vortex mixing for 5 min. (b) The curing characterization of the magnetic stirring mixing at 400 rpm for 30 min. The black and red number labels in the chart are curing thickness and curing time, respectively.

Different concentrations of the random MWCNTs in the photocurable polymer resin using the vortex and magnetic mixing method were examined for their curing depth properties. The concentration of the MWCNTs directly influences the curing parameter since the MWCNT particles scatter the projected light and further hinder the photopolymerization. As shown in Fig. 2a, the curing depth increased gradually as the concentration of MWCNTs was increased under the condition of vortex mixing; this is because the particles are inhomogeneously dispersed and take longer to solidify precisely to the desired shape. Different from vortex mixing, the curing depth is greatly reduced and gradually decreases with the increase of the proportion of MWCNTs for magnetic mixing (Fig. 2b). Moreover, the curing time required for the same concentration is longer than vortex mixing, which is caused by the light-shielding properties of the increasingly aggregated MWCNTs. Therefore, the trend of curing depth of the mixture under vortex mixing is completely different from that of magnetic stirring, and its characteristic is between pure resin and homogeneous polymer/MWCNT mixture. After observing the curing times and depths for these two different mixture techniques, the magnetic-stirred mixtures, which already have a better dispersion rate, show lower curing depths. The vortex mixture is overcured for the shortest printing time, whereas the magnetic-stirred mixtures are good at that rate and the curing depth can be fixed for the respective mixtures. This further helps us to proceed with this technique to prepare material to print with different concentrations.

Dynamic Alignment Under Electrical Field

While aligning MWCNTs under electric field, there is a need for voltage source, and it needs to be regulated (Fig. 3a). As the MWCNT is highly conductive, it can change its directions at microscale. When it is introduced into AC electric field, it aligns in the direction of the field. Under high voltage parameters, MWCNTs try to increasingly align, and then the small alignments observed can lead to formation of thicker chain-like structures in between the electrodes inside the resin. Some of the MWCNTs can also be observed depositing at the electrodes. This leads to the separation of MWCNTs from the resin, which is not good for printing. We recorded the dynamic arrangement process of MWCNTs with different mixing conditions under 100 V/mm AC electric field. Due to the large size of vortex stirring particles, they take a longer time to arrange, but the corresponding bundle size is larger and the connection between the particles is more obvious. As time goes on, the particles come together in a line, and more light passes through the mixture (Fig. 3b). Because an alternating current is used, the particles are arranged in situ rather than moving towards electrodes as they would under a direct current field. The use of an alternating current field greatly improves the stability of the arrangement. In contrast, magnetic stirring makes the particle dispersion more uniform, and the electrical conductivity of the mixture is enhanced (Fig. 3b). Besides, the magnetically stirred MWCNTs took much less time (30 s, Fig. 3c) to obtain the stable alignment of MWCNTs compared with vortex mixed MWCNTs (90 s, Fig. 3b).

The time taken for the alignment of MWCNTs in 0.5 wt.% mixture gradually decreased from 73 to 15 s as AC voltage increased from 0.5 kV to 2 kV because the high voltages activate the MWCNTs to align faster. The same phenomenon could be observed in the rest of the mixtures as the alignment time decreased from 58 s, 49 s, 42 s and 33 s to 12 s, 10 s, 10 s and 8 s for 1 wt.%, 1.5 wt.%, 2 wt.% and 2.5 wt.% mixtures, respectively (Fig. 3c). On observing the variation in time taken for the MWCNT mixtures for the same voltage of 0.5 kV, that is 33 s for 0.5 wt.% to 73 s for 2.5 wt.%, the higher the weight percentage of MWCNTs present in the mixture, the more time it takes for them to align at low voltages, and this gradually decreases with increase in the AC voltage. Notably, at 2 kV,

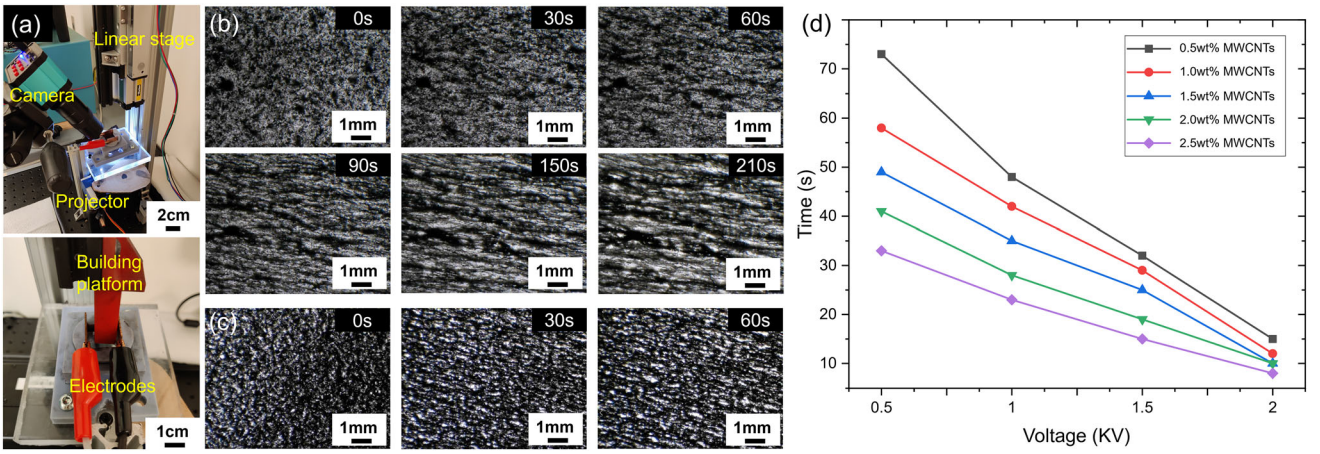

Fig. 3. Dynamic electric alignment of MWCNTs. (a) Electrically assisted vat photopolymerization set-up. (b) Alignment of vortex mixed MWCNT particles. (c) Alignment of magnetically stirred MWCNT particles. All the percentages of MWCNTs are 2.5 wt.%. (d) Electric field application time required for different voltages under different concentrations of MWCNTs.

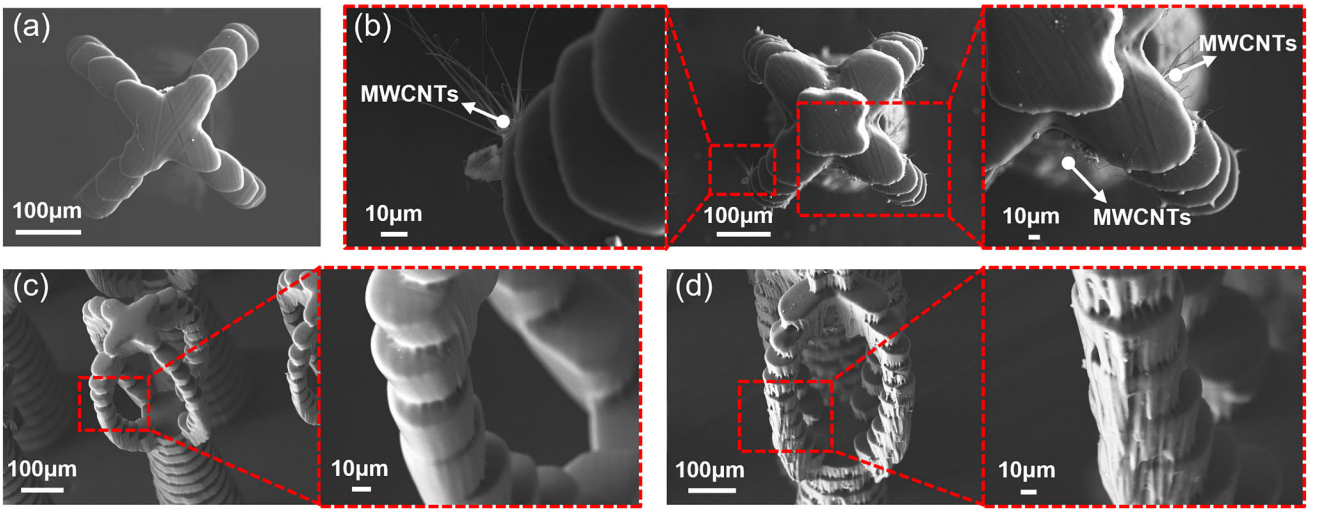

Fig. 4. Eggbeater-shaped structures made from pure resin and resin/MWCNT mixture. (a) Top view of structure made from pure resin. (b) Top and partial view of structure made from resin/MWCNT mixture. Side and partial view of the structure's head made from (c) pure resin and (d) resin/MWCNT mixture.

0.5 wt.% mixture takes 15 s and 2.5 wt.% takes 8 s to align, which is not a big difference.

e-VPP of Eggbeater Shaped Structures and Mechanical Performance Simulation

After studying the curing characteristics of the material and the dynamic alignment process of MWCNTs in an electric field, we printed the eggbeater structure using pure resin and resin/MWCNT mixture, where an electric field was applied to align the MWCNTs while printing the mixture. The top and side views of the structure printed with pure resin are shown in Fig. 4a,c. The partial view shows that the structure is complete as a whole, the surface is smooth, and there is no over-curing between layers. In contrast, after the addition of MWCNTs, the surface roughness of the structure increases, and its sides have many MWCNT fibers perpendicular to the surface, which benefits from the electric field applied during printing (Fig. 4b,d). This unevenness on the micrometer scale and roughness on the nanometer scale caused by MWCNT fibers synergistically enhance the superhydrophobic properties of the structure, which will be elucidated in the follow-up sections.

By adding gravity to the droplets, it was possible to mimic how water droplets would compress on a 3D-printed eggbeater structure. The model was designed in SolidWorks and simulated in COMSOL Multiphysics (Fig. 5a). According to Yang et al.'s

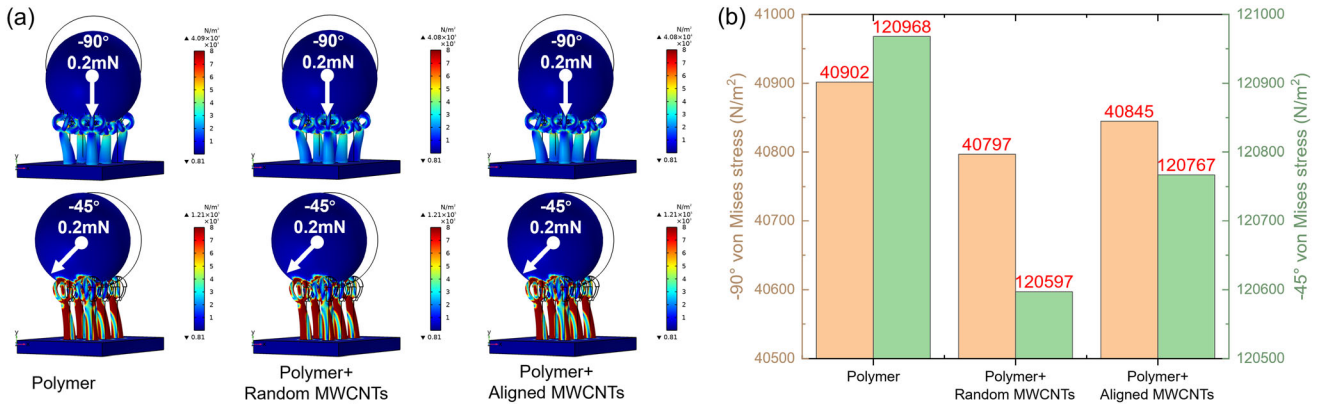

Fig. 5. Structural mechanical performance simulation. (a) Schematic diagram of the simulation of relative stress by COMSOL Multiphysics for the water droplet on the top of the superhydrophobic eggbeater arrays for different materials. (b) Maximum stress in different directions of applied force. The stress type in (a) is von Mises stress, and the unit is N/m^2.

work,[34] the modulus is set at 2.06 MPa, 4.13 MPa and 3.18 MPa for red resin, 1.5 wt.% MWCNT random mixture and aligned mixture, respectively. To simplify calculations, the composite is considered a continuum system, assuming the mechanical properties of the homogeneous MWCNT/resin composite to be isotropic. After arranging the internal particles, distinct simulation parameters are utilized in different directions for the composite, resulting in an anisotropic simulated model. The water droplet is assumed to be stationary, and the applied force is the gravity on the droplets to study the deformation of eggbeater arrays. To observe the deformation of eggbeater arrays in various directions, a side force was also applied. As shown in Fig. 5b, the red resin-made structure has stresses of 40.902 kPa, which are the highest for all the vertical drop simulations. This is because the structural strength of the structure made using pure photopolymer is low compared to the MWCNT mixture-made structures. The modulus increases with the help of these nanofillers, and the stresses induced are reduced to 40.797 kPa. Then, for the aligned mixture, the stress is slightly increased to 40.845 kPa. The stresses induced at 45° angle gradually decrease from 120.968 kPa, to 120.597 kPa, to 120.767 kPa for polymer resin MWCNTs in random and aligned orientation. The side force applied induces more stresses on these structures compared to the vertical drop, as shown in Fig. 5b, because the structures created using this e-VPP technique are structurally strong in the vertical direction, which means they can absorb more compressive forces.

Evaluation of Superhydrophobicity

To study the effect of spacing on superhydrophobicity, a series of structures was printed. The contact angle increases as the distance between the eggbeater structures widens (Fig. 6a). The increased surface area between the eggbeater tip and the water droplet is responsible for this. The eggbeater structure with more distance, on the other hand, does not have any hydrophobicity. This is due to the size of the water droplet that is dropped on these structures and its simultaneous distribution on each arm. The eggbeater arrays function best when there is a gap of 500 μm between them (Fig. 6b), considering the structures' superhydrophobicity and strength.

The contact angles go from 110.2° to 116.0° and 118.6° for 400 μm, 450 μm and 500 μm, respectively, according to Fig. 6b. Then, they decrease for 550 μm and 600 μm at 93.7° and 91.5° for the pure resin as the eggbeater structure cannot hold the drop on its heads. This trend is the same for the 0.5 wt.% MWCNT mixture. It reaches a peak at 500 μm with a CA of 127.4°, and for other gaps of 400 μm, 450 μm, 550 μm and 600 μm, the contact angles obtained are 123.8°, 125.7°, 96.5° and 92.3°, respectively. This explains why the contact angle reaches its peak at 500 μm gap between each individual eggbeater for both resins. So, further experiments with 1 wt.%, 1.5 wt.%, 2 wt.% and 2.5 wt.% MWCNT mixtures can be tested with the same geometry. This can help the random and aligned MWCNT mixtures to reach superhydrophobicity. The contact angles observed for 500 μm are higher for resin/0.5 wt.% MWCNT mixture compared to pure resin. Though they are not superhydrophobic, there is a hydrophobic behavior in these two models. So, for further tests and prints with different concentrations of MWCNTs, 500 μm gap is selected and tested for research purposes.

A 5-mm cube is designed and printed using e-VPP 3D printing with all the different mixtures of the resin, random and aligned with a layer thickness of 50 μm, to achieve a controlled layer thickness. All the mixtures of MWCNTs are aligned under electric field and are printed to obtain a set of samples to observe the microscale roughness of the printing that can be achieved with this form of 3D printing. This microscale roughness is an important factor in the contact angle measurement as the roughness

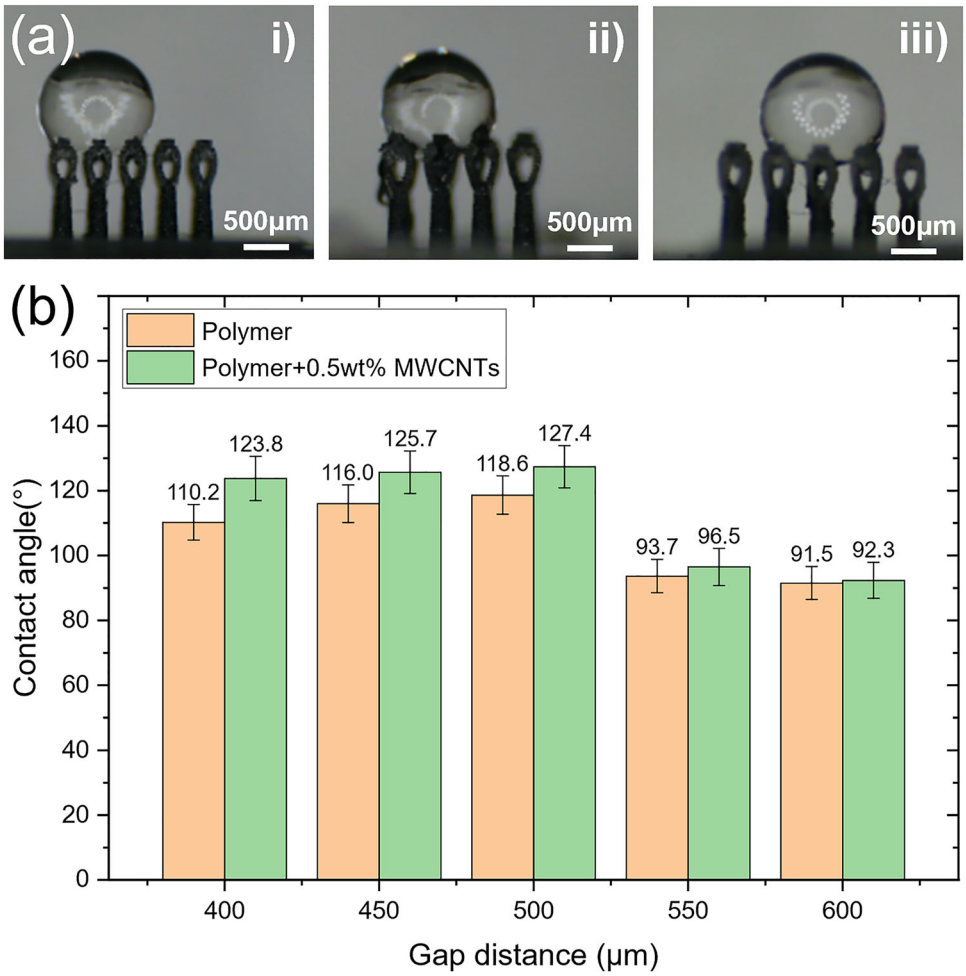

Fig. 6. Investigation of the relationship between different materials, contact angle and spacing. (a) Relationship between contact angle and spacing: (i) 400 μm, (ii) 450 μm and (iii) 500 μm. (b) Eggbeaters with 0.5 wt.% MWCNTs showing superhydrophobic properties for water droplet.

determines the hydrophobicity of a structure. All the mixtures of 0 wt.%, 0.5 wt.%, 1 wt.%, 1.5 wt.%, 2 wt.% and 2.5 wt.% MWCNTs, both randomly oriented and aligned mixtures, are used to print the 5-mm-long cube of length. All these samples are tested under a profilometer to measure the surface roughness within a single printed layer. All these cubes are printed under electric field with a constant voltage of 1 kV. This print roughness observed under the profilometer is considered as the microscale roughness that will be used in the manufacturing of superhydrophobic structures. When observed under profilometer, each individual layer can be seen like grooves with convex and concave surfaces, which tell us the roughness of each individual layer (Fig. 7c,d). Here, we have three different studies just for the roughness measurement for both the vortex- and magnetic-stirred mixtures. They are randomly oriented, and the aligned MWCNTs are in both horizontal orientation and vertical orientation, or the direction of electric field and the perpendicular direction to the electric field, respectively. Figure 7a,b shows all the different trends that were caused by random orientation, horizontal and vertical sides of aligned MWCNT under 1 kV for the mixtures of 0 wt.%, 0.5 wt.%, 1 wt.%, 1.5 wt.%, 2 wt.% and 2.5 wt.% MWCNT mixtures. Different curing times and voltages are used four different mixtures of MWCNTs to observe the roughness by keeping the curing depth constant at 50 μm.

For vortex mixture, the random MWCNTs have lower surface roughness in different concentrations, which means the random orientation of MWCNTs creates individual layers with low surface roughness at microscale. It is the same for magnetic state mixture as the surface roughness gradually increases as the MWCNT concentration raises from 0 wt.% to 2.5 wt.%. The roughness of 2.5 wt.% vortex mixture is 2.5 μm whereas magnetic state mixture is 4.2 μm. This explains that the roughness caused by printing these structures using magnetic stirring mixture is higher than the vortex mixture. This must be because the rate of dispersion off the magnetic-stirred mixture is better than for the vortex mixture. By observing the horizontal and vertical sides of MWCNT alignment, the trend is different from the random orientation. This could be

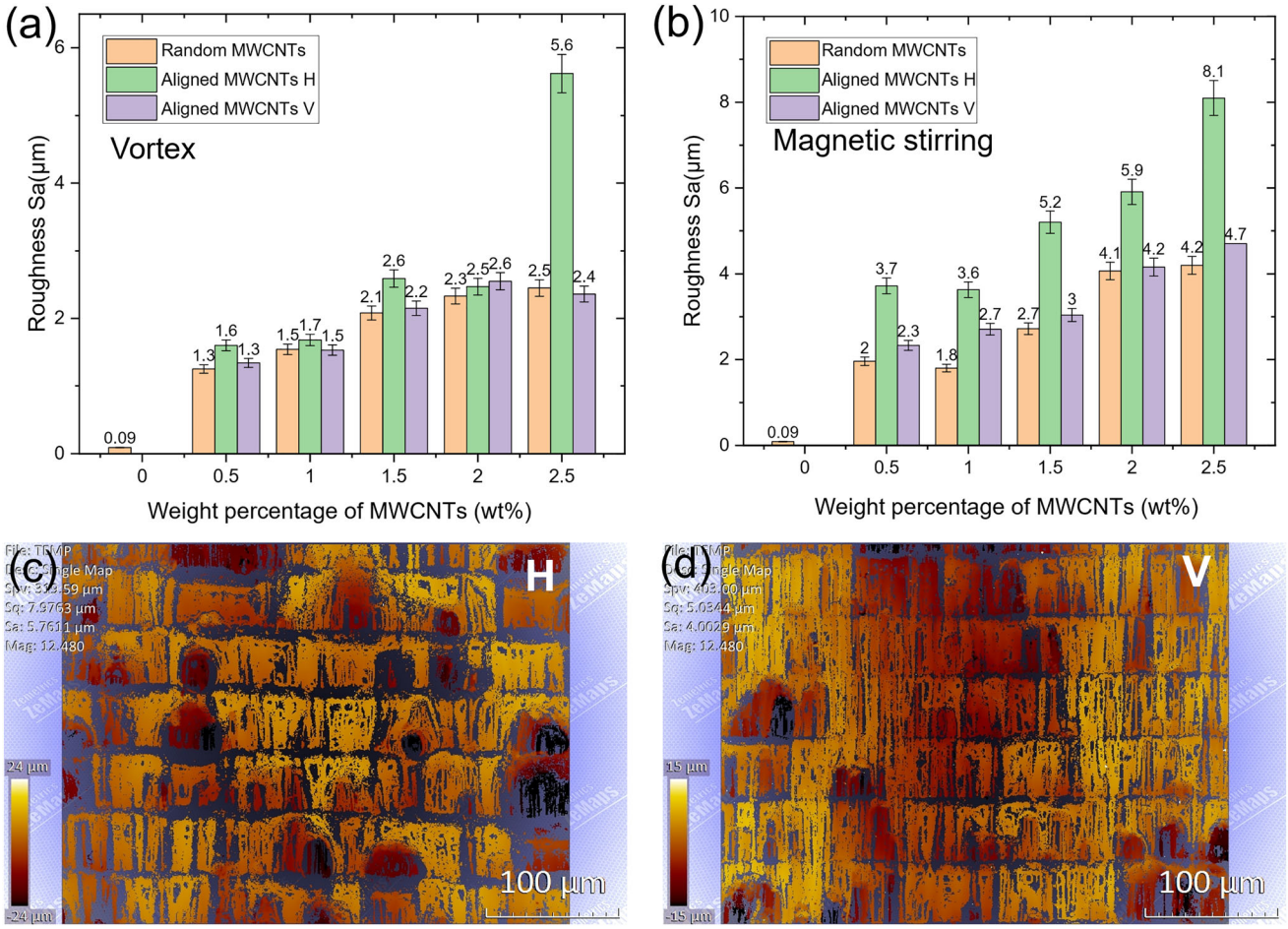

Fig. 7. Effect of dispersion conditions on surface roughness. (a) The surface roughness of the printed part using the material of vortex mixing for 5 min. (b) The surface roughness of the printed part using the material of magnetic stirring mixing at 400 rpm for 30 min. The data characterize surface roughness of the disorder state, the surface parallel (H) and perpendicular(V) to the alignment direction in (a, b). (c) Surface morphology of H-direction. (d) Surface morphology of V-direction. The material used in (c,d) is magnetic-stirred 1 wt.% MWCNTs at 400 rpm for 30 min.

because the higher percentages of MWCNTs present in the mixture causes more alignment, which leads to an increase in the surface roughness at micro-scale in both vortex- and magnetic-stirred mixtures. For the horizontal side of aligned MWCNTs, the roughness is 1.6 μm for 0.5 wt.% mixture and increases until 2.5 wt.% at 5.6 μm. The trend is almost the same for the magnetic state mixture where the roughness is observed at 3.7 μm for 0.5 wt.% and 3.6 μm at 1 wt.%, and it reaches highest of 8.1 μm at 2.5 wt.%. This also explains that the roughness observed for the alignment is higher in the magnetic-stirred mixture compared to the vortex mixture.

In the aligned MWCNTs, on the vertical side, the roughness measurements observed are almost like those on the horizontal side for both vortex- and magnetic-stirred mixtures but just slightly lower. It starts from 1.3 μm at 0.5 wt.%, reaches 2.6 μm at 2 wt.% and then decreases to 2.4 at 2.5 wt.% in vortex-mixed composite; this trend is almost similar to the horizontal alignment. Now, the magnetic-stirred mixture is also similar, but the roughness is a bit higher than the vortex mixture and starts at 2.3 μm for 0.5 wt.% and reaches 4.7 μm for 2.5 wt.%. The trends that are observed for the alignment of both horizontal and vertical mixtures of MWCNT for both the vortex and magnetic-stirred mixtures are similar and are gradually increased compared to the random MWCNT alignment, which also reaches the peak roughness at 2.5 wt.%. Thus, the rate of dispersion and the amount of MWCNT weight percentage added to the resin alter the roughness of the print for each individual layer when aligned under electric field.

The mixtures for different concentrations of MWCNTs from 0.5 wt.% to 2.5 wt.% are made using magnetic stirring method, and the eggbeater structures are made using these different concentrations. The contact angles are measured from the images taken while the water droplets of 5–7.5 μL (Fig. 8c) are placed above these structures. Then, the measured contact angles are observed and are shown in Fig. 8a. Comparing the contact angle from pure resin, there is an obvious difference when the MWCNTs are included. This shows that MWCNTs

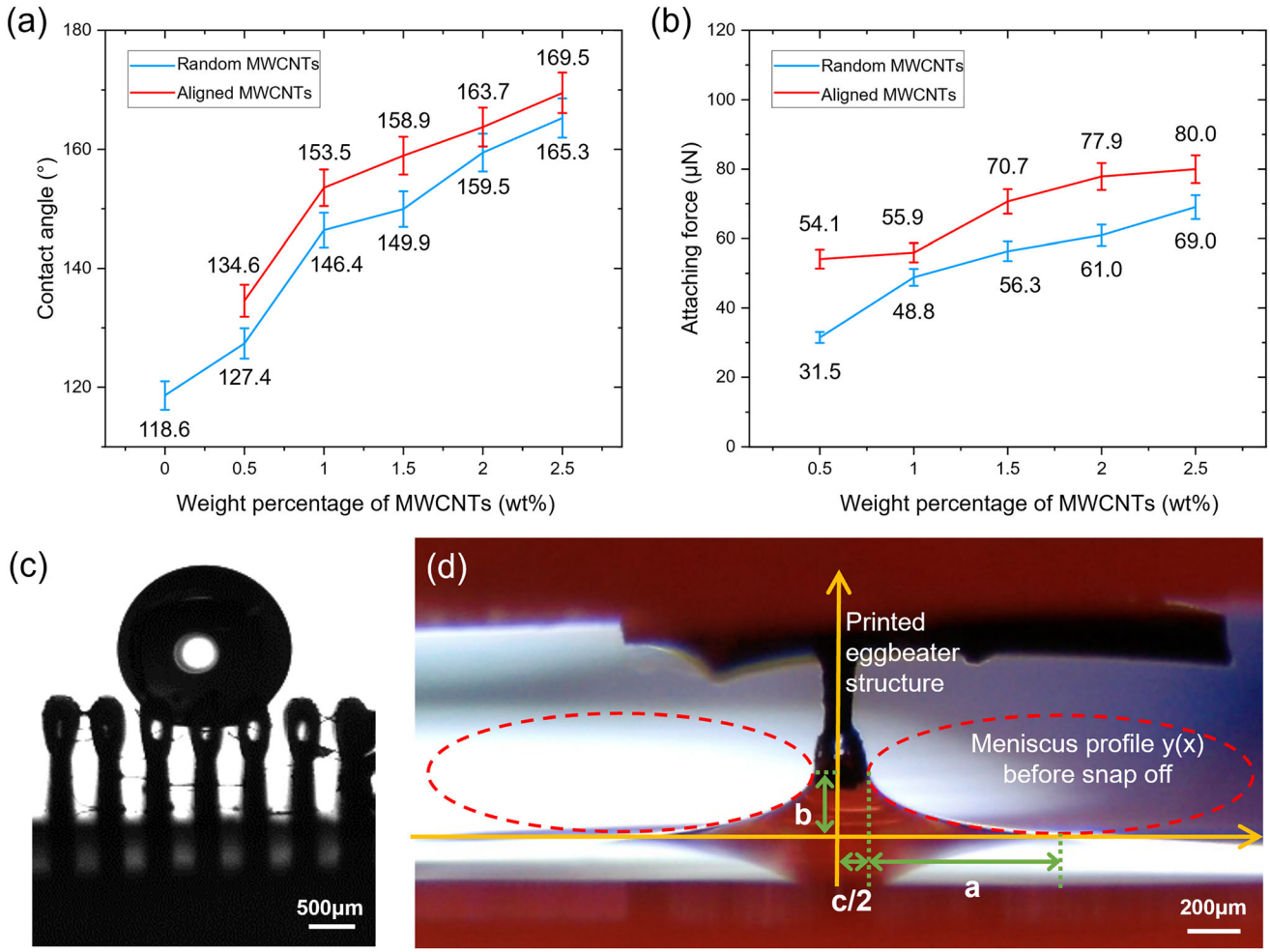

Fig. 8. Influence of MWCNT ration on superhydrophobicity. Effect of MWCNT concentration and alignment state on (a) contact angle and (b) attaching force. (c) Image of contact angle test. (d) Image of attaching force test.

improve the surface roughness of these structures and further help to improve their superhydrophobicity. The contact angle for the random and aligned mixtures of MWCNTs are measured using ImageJ software. The maximum contact angle can be observed for the aligned 2.5 wt.% MWCNT mixture with 169.5° and the next highest is observed with 165.3° for the random 2.5 wt.% MWCNT mixture. These results show that the alignment of MWCNTs could improve the contact angle of the structures, which increases the superhydrophobicity. The MWCNTs in the mixture act as nanofillers to increase the roughness at micro-scale and improve the contact angle and superhydrophobic properties.

As shown in Fig. 8d, the liquid forms a meniscus surface at the bottom of the structure, and its profile, the liquid volume and volume force can be fitted by the following formula:

$$y(x) = -\frac{b}{a}\sqrt{a^2 - \left(x - a - \frac{c}{2}\right)^2} + b \qquad (2)$$

$$V = 2\pi\left[\int_0^{c/2} x \cdot b\,dx + \int_{c/2}^{a+c/2} x \cdot y(x)\,dx\right] \qquad (3)$$

$$F_G = \rho V g \qquad (4)$$

where a, b and c are depicted in Fig. 8d; the V is volume of the liquid inside the meniscus surface, F_G is the volume force induced by the gravity, ρ is density of liquid, and g is gravitational acceleration.

As shown in Fig. 8b, the maximum attaching forces are observed for the aligned MWCNT structures. And the maximum force observed is for 2.5 wt.% MWCNT mixture, which is the maximum MWCNT weight percentage aligned in this experiment. The results showed that the adhesive force increased from low (31.5 μN) to high (69 μN) with an increase in the percentage of MWCNTs added to the resin. This growth is related to the alteration of the roughness in the microstructure scale and shape, which creates various sticky regions for water droplets on the surface. After aligning the

MWCNTs, the structure exhibits an overall better attaching force than the randomly distributed state. The results show that the printed eggbeater structure using the e-VPP 3D printing technique has a controlled attaching force for both the random and aligned MWCNT mixtures, but the attaching forces observed for the aligned MWCNTs are higher than the others by at least 5–20 μN at different concentrations.

CONCLUSION

The rough nano- and micro-scale hierarchical surface produces air pockets, which significantly reduces the solid–liquid interaction. The smaller solid–liquid contact area makes the surface more hydrophobic because it enables water droplets to become virtually perfectly spherical and easily slide off it. The wetting properties of the printed structure were tested in this study, and they were compared under random and aligned state with the same process parameters with different MWCNT percentages. The structure's wetting performance is primarily controlled by its composition, micro/nano-scale roughness and structural geometry. As a result of this study, one unique additive manufacturing technique has been presented to fabricate hierarchical superhydrophobic structures with controllable multi-scale roughness. Analysis and experimental validation have been done on the relationship among material qualities, manufacturing process parameters, and surface roughness and geometry parameters. Analytical models and experimental data were used to evaluate the impact of manufacturing parameters and material characteristics on the printed structure, including alignment state of the MWCNTs, the spacing of the structure, surface roughness and contact angle. Wetting characteristics of the hierarchical structures were also examined along with the mechanical properties like attaching forces. Results show that adding and aligning MWCNTs can enhance the structure's superhydrophobicity. The study supports the feasibility of creating multi-scale hierarchical surface structures inspired by biological systems by aligning MWCNTs under an electric field, which has a number of potential applications in water wheel propellers,[35] anisotropic water transport and water/oil separation.[36]

ACKNOWLEDGEMENTS

The authors acknowledge ASU Startup Funding, ASU FSE Strategic Interest Seed Funding, National Science Foundation (NSF grant no. CMMI-2114119) and the ASU core research facilities for the use of SEM electron microprobe analyzer.

FUNDING

ASU Startup Funding, ASU FSE Strategic Interest Seed Funding, National Science Foundation (NSF Grant no. CMMI-2114119).

CONFLICT OF INTEREST

The authors declare that they have no conflict of interest.

REFERENCES

1. A. Lafuma, and D. Quéré, *Nat. Mater.* 2, 457–460 https://doi.org/10.1038/nmat924 (2003).
2. R. Blossey, *Nat. Mater.* 2, 301–306 https://doi.org/10.1038/nmat856 (2003).
3. W. Barthlott, T. Schimmel, S. Wiersch, K. Koch, M. Brede, M. Barczewski, S. Walheim, A. Weis, A. Kaltenmaier, A. Leder, and H.F. Bohn, *Adv. Mater.* 22, 2325–2328 https://doi.org/10.1002/adma.200904411 (2010).
4. X. Yao, Y. Song, and L. Jiang, *Adv. Mater.* 23, 719–734 https://doi.org/10.1002/adma.201002689 (2011).
5. O. Tricinci, T. Terencio, B. Mazzolai, N.M. Pugno, F. Greco, and V. Mattoli, *ACS Appl. Mater. Interfaces.* 7, 25560–25567 https://doi.org/10.1021/acsami.5b07722 (2015).
6. D. Quéré, *Nat. Mater.* 1, 14–15 https://doi.org/10.1038/nmat715 (2002).
7. C. Yan, P. Jiang, X. Jia, and X. Wang, *Nanoscale* 12, 2924–2938 https://doi.org/10.1039/C9NR09620E (2020).
8. T. Tang, S. Alfarhan, K. Jin, and X. Li, *Adv. Funct. Mater.* 33, 2370029 https://doi.org/10.1002/adfm.202370029 (2023).
9. W. Gao, Y. Zhang, D. Ramanujan, K. Ramani, Y. Chen, C.B. Williams, C.C.L. Wang, Y.C. Shin, S. Zhang, and P.D. Zavattieri, *Comput. Aided Des.* 69, 65–89 https://doi.org/10.1016/j.cad.2015.04.001 (2015).
10. L. Tiwari, T. Tang, J. Rong, W. Shan, Y. Yang, and X. Li, *J. Mater. Sci. Technol. Res.* 9, 105–113 (2022).
11. Y. Yang, X. Song, X. Li, Z. Chen, C. Zhou, Q. Zhou, and Y. Chen, *Adv. Mater.* 30, 1706539 https://doi.org/10.1002/adma.201706539 (2018).
12. K. Koch, B. Bhushan, Y.C. Jung, and W. Barthlott, *Soft Matter* 5, 1386–1393 https://doi.org/10.1039/B818940D (2009).
13. A. Solga, Z. Cerman, B.F. Striffler, M. Spaeth, and W. Barthlott, *Bioinspir Biomim* 2, S126–S134 https://doi.org/10.1088/1748-3182/2/4/s02 (2007).
14. T. Tengteng, J. Dylan and L. Xiangjia, *Advances in 3D Printing*, ed. S. Dr. Ashutosh (IntechOpen, Rijeka, 2023), p Ch. 5.
15. W.-L. Min, B. Jiang, and P. Jiang, *Adv. Mater.* 20, 3914–3918 https://doi.org/10.1002/adma.200800791 (2008).
16. Z. Xue, S. Wang, L. Lin, L. Chen, M. Liu, L. Feng, and L. Jiang, *Adv. Mater.* 23, 4270–4273 https://doi.org/10.1002/adma.201102616 (2011).
17. F.D. Nicola, P. Castrucci, M. Scarselli, F. Nanni, I. Cacciotti, and M.D. Crescenzi, *Nanotechnology* 26, 145701 https://doi.org/10.1088/0957-4484/26/14/145701 (2015).
18. Y. Zhu, T. Tang, S. Zhao, D. Joralmon, Z. Poit, B. Ahire, S. Keshav, A.R. Raje, J. Blair, Z. Zhang, and X. Li, *Add. Manuf.* 52, 102682 https://doi.org/10.1016/j.addma.2022.102682 (2022).
19. Y. Yang, Z. Chen, X. Song, B. Zhu, T. Hsiai, P.-I. Wu, R. Xiong, J. Shi, Y. Chen, Q. Zhou, and K.K. Shung, *Nano Energy* 22, 414–421 https://doi.org/10.1016/j.nanoen.2016.02.045 (2016).
20. M. Jin, X. Feng, L. Feng, T. Sun, J. Zhai, T. Li, and L. Jiang, *Adv. Mater.* 17, 1977–1981 https://doi.org/10.1002/adma.200401726 (2005).
21. N. Zhao, Q. Xie, X. Kuang, S. Wang, Y. Li, X. Lu, S. Tan, J. Shen, X. Zhang, Y. Zhang, J. Xu, and C.C. Han, *Adv. Funct. Mater.* 17, 2739–2745 https://doi.org/10.1002/adfm.200601012 (2007).
22. Y. Zhu, J. Zhang, Y. Zheng, Z. Huang, L. Feng, and L. Jiang, *Adv. Funct. Mater.* 16, 568–574 https://doi.org/10.1002/adfm.200500624 (2006).
23. M.J. Hancock, K. Sekeroglu, and M.C. Demirel, *Adv. Funct. Mater.* 22, 2223–2234 https://doi.org/10.1002/adfm.201103017 (2012).

24. J. Yuan, X. Liu, O. Akbulut, J. Hu, S.L. Suib, J. Kong, and F. Stellacci, *Nat. Nanotechnol.* 3, 332–336 https://doi.org/10.1038/nnano.2008.136 (2008).
25. Y. Lai, X. Gao, H. Zhuang, J. Huang, C. Lin, and L. Jiang, *Adv. Mater.* 21, 3799–3803 https://doi.org/10.1002/adma.200900686 (2009).
26. X.J. Feng, and L. Jiang, *Adv. Mater.* 18, 3063–3078 https://doi.org/10.1002/adma.200501961 (2006).
27. Y. Li, W. Wang, F. Wu, and R.K. Kankala, *Front. Mater.* https://doi.org/10.3389/fmats.2022.1118943 (2023).
28. S.H. Siddique, P.J. Hazell, H. Wang, J.P. Escobedo, and A.A.H. Ameri, *Add. Manuf.* 58, 103051 https://doi.org/10.1016/j.addma.2022.103051 (2022).
29. X. Zhou, L. Ren, Q. Liu, Z. Song, Q. Wu, Y. He, B. Li, and L. Ren, *Macromol. Biosci.* 22, 2100332 https://doi.org/10.1002/mabi.202100332 (2022).
30. D. Joralmon, S. Alfarhan, S. Kim, T. Tang, K. Jin, and X. Li, *ACS Appl. Polym. Materials* 4, 2951–2959 https://doi.org/10.1021/acsapm.2c00322 (2022).
31. Issempa, *Wikimedia Commons* (2013, Internet https://commons.wikimedia.org/wiki/File:Bild_von_Salvinia_molesta.JPG).
32. D. Gandyra, S. Walheim, S. Gorb, P. Ditsche, W. Barthlott, and T. Schimmel, *Small* 16, 2003425 https://doi.org/10.1002/smll.202003425 (2020).
33. T. Tang, B. Ahire, and X. Li, *J. Manuf. Sci. Eng.* 145, 8892 https://doi.org/10.1115/1.4055793 (2022).
34. Y. Yang, Z. Chen, X. Song, Z. Zhang, J. Zhang, K.K. Shung, Q. Zhou, and Y. Chen, *Adv. Mater.* 29, 1605750 https://doi.org/10.1002/adma.201605750 (2017).
35. T. Tang, S. Alfarhan, K. Jin, and X. Li, *Adv. Funct. Mater.* https://doi.org/10.1002/adfm.202211602 (2022).
36. C. Zeiger, I.C. Rodrigues da Silva, M. Mail, M.N. Kavalenka, W. Barthlott, and H. Hölscher, *Bioinspir Biomim* 11, 056003 https://doi.org/10.1088/1748-3190/11/5/056003 (2016).